



Direct electrical detection of hybridization at DNA-modified silicon surfaces

Wei Cai^a, John R. Peck^b, Daniel W. van der Weide^b, Robert J. Hamers^{a,*}

^a Department of Chemistry, University of Wisconsin-Madison, 1101 University Avenue, Madison, WI 53706, USA

^b Department of Electrical and Computer Engineering, University of Wisconsin-Madison, Engineering Hall, Madison, WI 53706, USA

Received 10 June 2003; received in revised form 23 September 2003; accepted 24 September 2003

Abstract

Electrochemical impedance spectroscopy was used to investigate the changes in interfacial electrical properties that arise when DNA-modified Si(1 1 1) surfaces are exposed to solution-phase DNA oligonucleotides with complementary and non-complementary sequences. The n- and p-type silicon(1 1 1) samples were covalently linked to DNA molecules via direct Si–C linkages without any intervening oxide layer. Exposure to solutions containing DNA oligonucleotides with the complementary sequence produced significant changes in both real and imaginary components of the electrical impedance, while exposure to DNA with non-complementary sequences generated negligible responses. These changes in electrical properties were corroborated with fluorescence measurements and were reproduced in multiple hybridization–denaturation cycles. The ability to detect DNA hybridization is strongly frequency-dependent. Modeling of the response and comparison of results on different silicon bulk doping shows that the sensitivity to DNA hybridization arises from DNA-induced changes in the resistance of the silicon substrate and the resistance of the molecular layers.

© 2003 Elsevier B.V. All rights reserved.

Keywords: Impedance spectroscopy; DNA; Hybridization; Sensor; Silicon; Electrical detection

1. Introduction

Surface-based methods for detection of biological molecules such as DNA and proteins have revolutionized biological detection (Fodor et al., 1993; Heller, 2002). However, only limited use has been made of the electrical properties of biologically-modified interfaces as a basis for biological sensing (Alfonta and Willner, 2001; Bardea et al., 1999; Boon et al., 2000; Cloarec et al., 2002; Gooding, 2002; Kharitonov et al., 2001; Korri-Youssoufi et al., 1997; Murphy et al., 1993; Patolsky et al., 2001; Popovich et al., 2002; Souteyrand et al., 1997; Vercoutere and Akeson, 2002; Wang, 2002; Willner and Willner, 2001; Yu et al., 2001). Because silicon is the basis for most micro-electronic devices such as amplifiers and microprocessors, development of biosensors that are directly integrated with silicon are particularly desirable. Most studies of biological interfaces to silicon have used SiO₂ as an intermediate

(Berggren et al., 2001; Cloarec et al., 2002; Souteyrand et al., 1997). There has recently been great interest in chemical and biochemical modification of silicon via direct Si–C bond formation, without involving an oxide intermediate (Buriak, 1999; Lin et al., 2002; Linford et al., 1995; Strother et al., 2000a,b; Wagner et al., 1997). Previous studies have shown that when direct Si–C bond formation is used as a starting point for DNA attachment, the resulting surfaces exhibit high selectivity and good stability (Lin et al., 2002; Strother et al., 2000a,b).

Here, we report investigations of the changes in electrical impedance that occur when silicon surfaces modified with DNA using direct Si–C bond formation chemistry are exposed to complementary and non-complementary DNA molecules in solution. Our results show clear, reversible changes in impedance that are associated with hybridization and are confirmed by fluorescence measurements. A comparison between n- and p-type substrates shows that the impedance changes arise in part from a field-induced effect in the silicon substrate. These results indicate that it should be possible to fabricate field-effect biosensing devices entirely via wet chemical procedures.

* Corresponding author. Tel.: +1-608-262-6371; fax: +1-608-262-0453.

E-mail address: rjhamers@facstaff.wisc.edu (R.J. Hamers).

2. Experimental

The electrochemical detection system, depicted in Fig. 1, is based on a three-electrode electrochemical cell containing a DNA-modified Si sample as a working electrode, a Ag/AgCl reference electrode, and a Pt counter-electrode. A polydimethylsiloxane (PDMS) fluid cell ($\sim 5 \mu\text{l}$ volume) containing an embedded Ag/AgCl reference electrode is pressure-sealed between the DNA-modified Si sample (8 mm \times 4 mm) and the Pt counter-electrode. Impedance spectra were measured using a three-electrode potentiostat (Solartron model 1287) coupled to an impedance analyzer (Solartron model 1260). All electrochemical potentials discussed here are with respect to the saturated Ag/AgCl reference electrode.

Results reported here used three types of (1 1 1)-oriented silicon samples. Most experiments were performed using heavily doped, n-type Si samples (resistivity = 0.005 Ω cm). Experiments were also performed using lightly-doped n-type samples (phosphorus-doped, 5 Ω cm) and p-type samples (boron-doped, 0.1 Ω cm). The samples were immersed into 40% NH_4F solution to produce hydrogen-terminated Si(1 1 1) surfaces (Higashi et al., 1990). These H-terminated samples were covered with a thin film of an aminoalkene (10-amino-1-ene) that was protected with the *t*-butyloxycarbonyl (*t*-BOC) group, and the liquid-covered surface was illuminated with 254 nm ultraviolet light (0.35 mW/cm²) for ~ 2 h under an atmosphere of dry nitrogen. Deprotection using 50% trifluoroacetic acid produces a surface terminated with primary amine groups. Thiol-modified oligonucleotides were then linked to these amine groups using the heterobifunctional cross-linker sulfo-succinimidyl-4-(*N*-maleimidomethyl)cyclohexane-1-

carboxylate purchased from Pierce Chemical. Previous studies have shown that this procedure yields DNA-modified Si(1 1 1) samples that exhibit high selectivity toward complementary versus non-complementary sequences in hybridization experiments, and that are stable under repeated cycles of hybridization and denaturation (Strother et al., 2000a,b).

Experiments were conducted using several different sequences for the surface-immobilized “probe” molecule and the solution-phase “target” molecules. The data presented here were obtained using an immobilized probe molecule with sequence 5'-HS-C₆H₁₂-T₁₅AACGATCGAGCTGCAA-3' (S1) and target molecules with sequences 5'-TTGCAGCTCGATCGTT-3' (S2) and 5'-TTGCTCCTGCATCGTT-3' (S3). Sequences S1 and S2 are perfect complements, while S1 and S3 are four-base mismatches. To isolate the changes in electrical response that can be directly associated with hybridization, most experiments involved a comparison of the responses produced when the DNA-modified silicon surfaces were exposed to the complementary (S2) versus a non-complementary (S3) sequence. In some cases, S2 and S3 were labeled with fluorescein at the 5'-end to enable the electrical signals to be directly corroborated the electrical measurements with fluorescence measurements. However, equivalent electrical signals were also observed using target molecules without fluorescent labels. Hybridization experiments and impedance spectroscopy measurements were all performed in a standard hybridization buffer (HB) consisting of 0.3 M NaCl, 0.02 M Na₃PO₄, 0.002 M ethylenediaminetetraacetic acid, and 0.2% sodium dodecyl sulfate. Denaturation was achieved by immersing in 30 mM KCl (adjusted to pH 13 using KOH) for 5 min, followed by rinsing with water and then with hybridization buffer.

3. Results and discussion

3.1. Impedance changes induced by complementary and non-complementary sequences

Fig. 2 shows the electrochemical response of a DNA-modified Si electrode measured at 0 V (versus Ag/AgCl) with a 5 mV root-mean-square sinusoidal modulation. For a given applied potential $V = V_0 + V_{\text{mod}} \cos(\omega t)$, the impedance can be expressed as a complex number $Z = Z' + jZ''$, where $j = \sqrt{-1}$. The individual logarithmic graphs in Fig. 2a and b show the real (in-phase, Z') and the imaginary (out-of-phase, Z'') components of the impedance.

In Fig. 2, the curves A1, B1, and C1 show the electrical response from 100 Hz to 500 kHz when the hybridization buffer was pumped through the flow cell. A 3 μM solution of the complementary DNA sequence S2 in HB was then introduced into the cell. After 20 min incubation, the fluid cell was flushed with HB for 5 min and the impedance data were recorded again, yielding traces A2, B2, and C2 in Fig. 2. A comparison of traces “1” and “2” shows that both the real and imaginary parts of the complex impedance

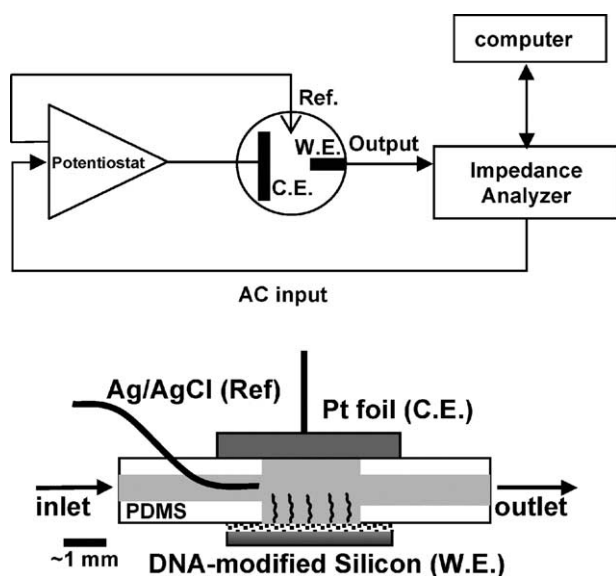


Fig. 1. Instrument setup and schematic of the three-electrode electrochemical fluid cell. The DNA-modified silicon sample is the working electrode (W.E.), while a platinum foil is used as the counter-electrode (C.E.).

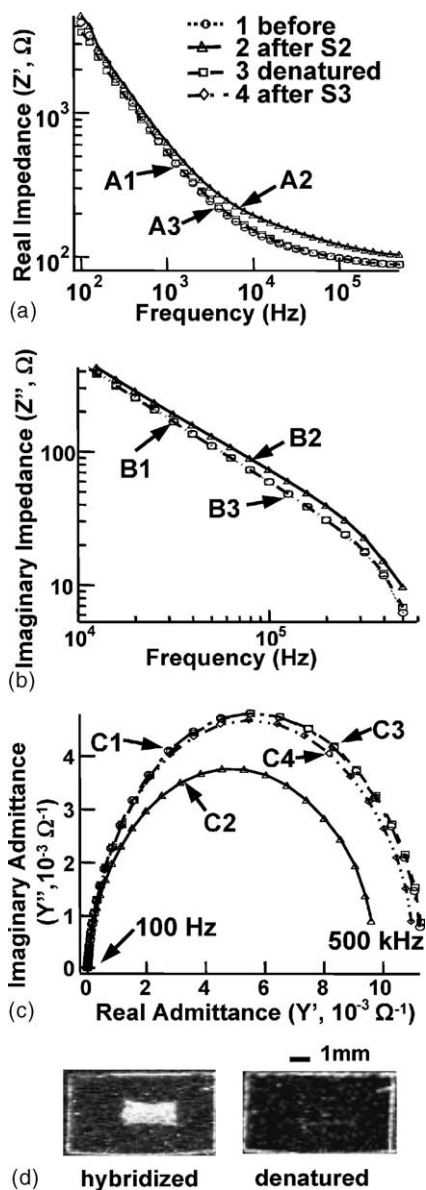


Fig. 2. Impedance and fluorescence data for DNA-modified Si(111) surface at various stages of hybridization and denaturation. (a) Real part of the complex impedance of Si(111) surface after covalent attachment of single-stranded DNA, after exposure to complementary sequence (S2), and after denaturation. Detailed procedure described in text. (b) Imaginary part of the complex impedance of the same sample as in (a). (c) Plot of the real vs. imaginary part of the complex admittance as a function of frequency. Trace C4 is impedance of the sample that was exposed to a mismatched sequence (S3) after denaturation step. (d) Fluorescence image (white: high intensity) of the Si electrode after hybridization (left) and after denaturation (right). The bright region in the center is the part of the sample that was exposed to the DNA solution in the electrochemical cell.

increase upon hybridization with the complementary sequence. These changes are difficult to see at low frequencies, but become apparent at frequencies higher than approximately 1 kHz. Because at these frequencies the total impedance is small, the hybridization-induced changes in electrical properties are more clearly observed by plotting

the real versus imaginary components of the complex admittance, $Y' = \text{Re}(1/Z) = (Z'/|Z|^2)$, $Y'' = \text{Im}(1/Z) = -Z''/|Z|^2$ as a function of frequency (Cole and Cole, 1941; Macdonald, 1987), as shown in Fig. 2c.

To confirm whether or not the observed electrical variations arise from DNA hybridization, the impedance of this same sample was measured after denaturation (as described earlier). The electrical response of the denatured sample (traces A3, B3, and C3) is almost identical to that of the starting surface (traces A1, B1, and C1). This similarity shows that denaturation returns the surface to a state that is electrically the same as the starting surface.

To test whether the changes in electrical properties depend specifically on the sequence of the solution-phase target molecule, the same Si electrode was then incubated in a 3 μM solution of the non-complementary oligonucleotides, S3, for 20 min and then flushed with HB. The resulting spectrum (Fig. 2c, trace C4) is nearly identical to that of the starting surface (Fig. 2c, trace C1). The impedance of the mismatched sequence is not shown in Fig. 2a or b, because the data are almost completely overlapped with traces A1 and B1 on the logarithmic scale. Thus, we conclude that the interaction of the surface-bound probe molecules with non-complementary oligonucleotides in solution yields electrical characteristics indistinguishable from those of the denatured surface.

3.2. Stability and repeatability

To test the stability and reproducibility of the electrical response, a series of measurements was performed on a sample that was sequentially incubated with either complementary sequence S2 or non-complementary sequence S3. In each cycle, the sample was incubated for 20 min with the DNA-containing solution of S2 or S3. This solution was then flushed out and the impedance spectrum was recorded in hybridization buffer. The sample was denatured between measurements. During four repeated cycles (four measurements with S2, four measurements with S3), these experiments showed that incubating in S2 yielded an average increase of $23 \pm 1\%$ in Z' and $15 \pm 1\%$ in $|Z''|$ at 100 kHz compared with the denatured surface, while incubating in S3 solution yielded increases of only $5 \pm 3\%$ in Z' and $8 \pm 1\%$ in $|Z''|$ compared with the denatured surface. These experimental data show that the changes in electrical response are well outside of any statistical fluctuations. Although individual sensor elements retain their sensitivity for repeated cycles of hybridization and denaturation over time periods of hours, some loss in sensitivity is observed over longer periods of time; the nature of this long-term degradation is still under investigation.

Along with the electrical measurements shown in Fig. 2, we measured the fluorescence intensity at 530 nm from the fluorescein-labeled targets. Fig. 2d shows a sample that was hybridized in the electrochemical cell, electrically characterized, removed, and then imaged. This sample (labeled

“hybridized”) shows high fluorescence intensity in a rectangular region near the center where it was exposed to the DNA in the cell. This same sample was then returned to the cell, denatured, electrically characterized, and removed again for imaging, yielding the image in Fig. 2d, labeled “denatured”. It should be noted that these images were obtained on the *same* sample and as part of the *same* experiment as the data shown in Fig. 2a–c. The close correspondence between the electrical data and the fluorescence data shows that impedance shifts arise from the hybridization of DNA to the surface-bound probe molecules.

3.3. Potential-dependent impedance measurements

While the data in Fig. 2 were obtained at a potential of 0 V versus Ag/AgCl, Fig. 3a shows how hybridization influences the impedance over a range of potentials from -0.6 to $+0.6$ V at a fixed frequency of 1 kHz. The potential-dependent impedance spectroscopy of silicon is quite complicated because of the electrical double-layer, semiconductor space-charge region, and the presence of interface states (Memming and Schwandt, 1966) and will not be discussed in detail here. However, the increase in magnitude of both real and imaginary components of the impedance as the potential is increased from -0.5 to $+0.2$ V on the n-type sample can be attributed to the formation of a depletion region with increased resistance and decreased capacitance; these changes indicate that the surface Fermi level is not pinned at a fixed value. Incubation with the complementary sequence S2 produces an increase in both the real and imaginary components of the impedance over the entire potential range and also shows a positive shift of ~ 50 mV, while the non-complementary sequence S3 elicits only an insignificant response. For comparison, Fig. 3 also shows the real part of the impedance measured at 100 kHz on samples prepared by modifying lightly-doped n-type silicon (Fig. 3b) and p-type silicon (Fig. 3c) substrates with DNA using the same procedure. While the shape of the impedance versus potential plot from lightly-doped sample (Fig. 3b) is different from that of the heavily-doped sample (Fig. 3a), a significant increase in real impedance is observed upon incubating with DNA. In contrast, when a p-type sample is used (Fig. 3c), hybridization with the complementary sequence causes the impedance to *decrease*. This doping dependence on the direction of impedance changes upon hybridization demonstrates that DNA hybridization at the electrode surfaces causes the electric field to change in the underlying silicon.

3.4. Electrical circuit modeling

In order to understand the physical basis of the impedance changes, the response of the interface was compared with a variety of different equivalent circuit models. While a number of models were investigated, the circuit shown in Fig. 4 provides a good fit to the data with a reasonable number of

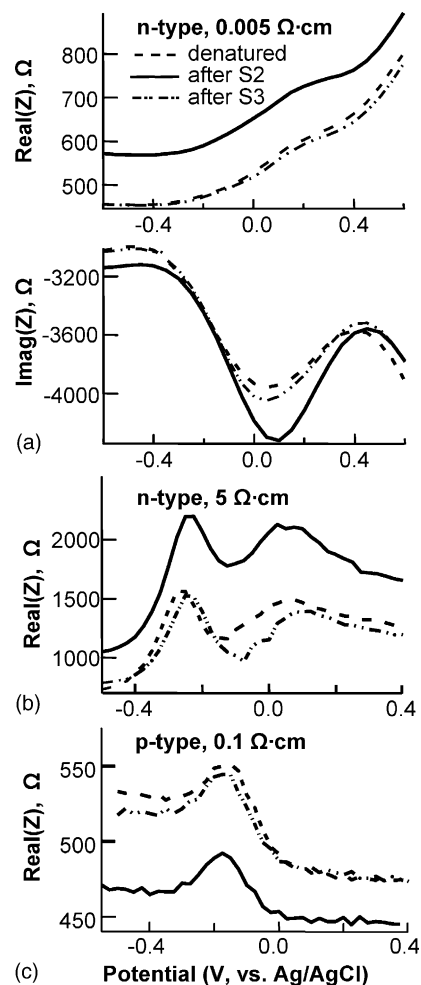


Fig. 3. Comparison of impedance data as a function of the applied electrochemical potential, from DNA-modified Si(111) samples with different bulk doping. In each case, data are shown from a denatured sample, after exposure to the complementary sequence S2, and after exposure to the non-complementary sequence S3. (a) The n-type, heavily-doped sample, $0.005 \Omega \text{ cm}$ resistivity, showing both real part (upper panel) and imaginary part (lower panel) of the complex impedance at 1 kHz ac. (b) The n-type, lightly-doped sample, $5 \Omega \text{ cm}$ resistivity, real part of the impedance at 100 kHz. (c) The p-type, heavily-doped sample, $0.1 \Omega \text{ cm}$ resistivity, real part of the impedance at 100 kHz.

circuit elements. This equivalent circuit consists of the capacitor C_{org} of the organic modification layer (including the DNA layer), and a leakage resistance R_{leak} that reflects penetration of the electrolyte through the molecular layer. The electrical double-layer is represented by a constant-phase element (CPE) and a parallel resistance R_{dl} . Finally, the silicon substrate is represented by a resistance R_{Si} in parallel with and capacitance C_{Si} , reflecting the properties of the space-charge region of the silicon. The thickness of the diffuse layer can be estimated from Gouy–Chapman–Stern theory and is approximately 1 nm under the conditions used in our experiments (Bard and Faulkner, 2001). Because this thickness is close to that of the aminoalkene layer (~ 1.6 nm) but smaller than the overall length of the surface-tethered

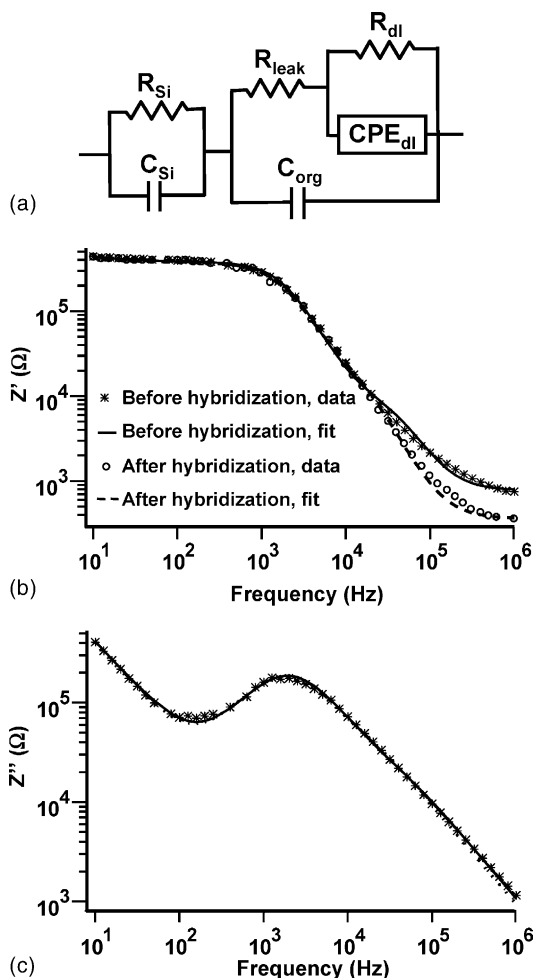


Fig. 4. Fitting of experimental data to equivalent circuit model. (a) The equivalent circuit used to fit the impedance data. (b) Experimental data and fit to the real part of the impedance before and after hybridizing to the complementary sequence S2. (c) Experimental data and fit to the imaginary part of the impedance, before and after hybridizing to the complementary sequence S2.

DNA molecule, the double-layer is not a well-defined discrete element. However, for the purposes of modeling, we have found that modeling the double-layer as depicted in Fig. 4, provides a good fit with a minimum number of free parameters. When fitting the experimental data, one set of fit parameters was used to fit both the real and imaginary parts of the impedance simultaneously.

Analysis of the impedance data using this circuit shows that at high frequencies ($>10^3$ Hz) where the sensitivity

to DNA hybridization is highest, the overall impedance is primarily controlled by the silicon space-charge region (R_{Si} and C_{Si}) and the resistance of the molecular layer, R_{leak} , in amounts that depend on the doping of the sample and the frequency of interest. Table 1 shows the numerical values of these parameters before and after hybridization with complementary DNA for lightly-doped n-type and heavily-doped p-type samples. Detailed analysis shows that for lightly-doped samples R_{Si} is larger and C_{Si} is smaller, making the resistive contribution of the silicon the dominant factor in the overall impedance. At higher doping levels, the smaller value of R_{Si} and large C_{Si} decrease the impedance of the silicon substrate, so the total impedance becomes more sensitive to R_{leak} . That the resistive elements primarily control the impedance at high frequencies can be easily seen in Fig. 2, from the fact that the real impedance is larger than the imaginary impedance at frequencies $>10^5$ Hz. Because the silicon and double-layer impedances are comparable in size at high frequencies, where DNA hybridization is most easily detected, separating the individual contributions is difficult. However, it is clear that under the conditions where DNA hybridization can be easily detected, the total impedance is controlled by R_{Si} , C_{Si} , and R_{leak} . At lower frequencies (less than ~ 1 kHz), the overall impedance is controlled by other circuit elements such as the solution double-layer, that provide less sensitivity to DNA hybridization.

To optimize the sensitivity of DNA detection, it is important to understand what factors control the total impedance and also what elements *change* in response to DNA hybridization. Fig. 2c shows that at 500 kHz the *change* in impedance due to DNA hybridization is apparent only on the real part of the impedance, shifting the 500 kHz data point parallel to the real (horizontal) axis. In general, we find that on n-type samples, both R_{Si} and R_{leak} increase upon hybridization, while on p-type samples both R_{Si} and R_{leak} decrease upon hybridization. Specific values for $5 \Omega \text{ cm}$ n-type and $0.1 \Omega \text{ cm}$ p-type samples are shown in Table 1. However, these trends were observed on all samples (n- and p-type doping levels from 0.005 to $10 \Omega \text{ cm}$) that we have investigated. The changes in R_{Si} are easily explained on the basis of the negative charge of DNA. As a negatively-charged DNA molecule approaches the interface, it repels the electrons in the adjacent semiconductor, leading to an upward band-bending. Since on n-type the majority carriers are electrons, the upward band-bending represents a decrease in the density of majority carriers in the semiconductor space-charge region, which in turn leads

Table 1
Numerical results of circuit elements obtained after analyzing impedance data using equivalent circuit shown in Fig. 4

	n-type (P-doped), $5 \Omega \text{ cm}$ resistivity			p-type (P-doped), $0.1 \Omega \text{ cm}$ resistivity		
	R_{leak} (k Ω)	R_{Si} (k Ω)	C_{Si} ($\times 10^{-10}$ F)	R_{leak} (k Ω)	R_{Si} (k Ω)	C_{Si} ($\times 10^{-10}$ F)
Before hybridization	0.55 ± 0.07	358 ± 6	1.94 ± 0.03	0.25 ± 0.02	57.4 ± 0.7	2.58 ± 0.03
After hybridization	1.26 ± 0.09	367 ± 7	1.89 ± 0.03	0.21 ± 0.01	55.3 ± 0.3	2.55 ± 0.01

to an increased resistance. Conversely, on p-type silicon the majority carriers are holes; in this case the upward band-bending represents an increase in the majority carrier density and a decreased resistance of the space-charge region. These field-effects are well known and can be used as the basis for field-effect devices (Cloarec et al., 2002; Fritz et al., 2002; Souteyrand et al., 1997).

Our data shows that DNA hybridization also changes the conductivity through the molecular layer, R_{leak} . We believe that the effect here can be explained by a similar field effect that operates in the electrolyte solution. Since n- and p-type Si have different bulk Fermi levels, the nature of the electrolytic double-layer at their interfaces will necessarily be different, and this would be expected to affect the migration of ions through the double-layer. Previous studies have reported that DNA hybridization at DNA-modified gold surfaces increased the resistance associated with electron transfer to ferricyanide/ferricyanide ($\text{Fe}(\text{CN})_6^{3-}/\text{Fe}(\text{CN})_6^{4-}$) redox couple (Alfonta and Willner, 2001; Bardea et al., 1999). These earlier studies attributed the increased resistance to the electrostatic repulsion between the negatively-charged hybridized DNA molecules and the negatively-charged redox molecules in solution. Although in our measurements the use of high-frequency measurements negates the need for auxiliary redox agents, the migration of ionic species in the buffer solution through the molecular layers is still expected to be affected by the interfacial charge distribution. Our data indicates that the electric field resulting from hybridization of DNA at the surface affects the ions in solution (as reflected in R_{leak}) and also affects the semiconductor space-charge region (as reflected in R_{Si}).

4. Conclusions

The results presented here show that the use of direct Si–C bond formation as the basis for DNA functionalization leads to good biomolecular recognition capabilities and can be used as the basis for direct electrical detection of DNA hybridization using impedance spectroscopy. While most previous studies have added redox agents to provide a pathway for continuous current flow, our results show that by operating at the open circuit potential and using impedance measurements at higher frequencies, it is possible to directly detect DNA hybridization directly in hybridization buffer, without any added redox agents. Unlike measurements of the overall changes in dc conductivity, ac impedance measurements can be performed with no direct current flowing through the sample, thereby minimizing the potential for modifying or damaging the biomolecular layers. Because the total impedance is affected by the substrate, by the molecular and biomolecular layers, and by the electrolytes, identifying conditions under which DNA hybridization can be detected requires understanding how these different factors contribute to the overall impedance. Our results show that the electrical sensing at these layers is obtained at higher

frequency under conditions where the total impedance is dominated by the silicon and the resistance of the molecular layers. While more work will be needed to optimize sensitivity and more fully understand the signal transduction process, the results reported here demonstrate the viability of combining direct Si–C bond formation chemistry with direct electrical measurements of interfacial impedance to detect DNA hybridization at silicon surfaces.

Acknowledgements

The authors express our thanks to Prof. Lloyd M. Smith for helpful discussions. This work was supported by the Wisconsin Alumni Research Foundation, the US Office of Naval Research Grant N00014-01-1-0654, and the National Science Foundation Grants CHE0071385 and DMR0210806. Any opinions, findings, and conclusions or recommendations expressed in this publication are those of the authors and do not necessarily reflect the views of these agencies.

References

- Alfonta, L., Willner, I., 2001. Electronic transduction of biocatalytic transformations on nucleic acid-functionalized surfaces. *Chem. Commun.* 16, 1492–1493.
- Bard, A.J., Faulkner, L.R., 2001. *Electrochemical Methods: Fundamentals and Applications*, 2nd ed. Wiley, New York, pp. 534–579.
- Bardea, A., Patolsky, F., Dagan, A., Willner, I., 1999. Sensing and amplification of oligonucleotide–DNA interactions by means of impedance spectroscopy: a route to a Tay-Sachs sensor. *Chem. Commun.* 1, 21–22.
- Berggren, C., Bjarnason, B., Johansson, G., 2001. Capacitive biosensors. *Electroanalysis* 13, 173–180.
- Boon, E.M., Ceres, D.M., Drummond, T.G., Hill, M.G., Barton, J.K., 2000. Mutation detection by electrocatalysis at DNA-modified electrodes. *Nat. Biotechnol.* 18, 1096–1100.
- Buriak, J.M., 1999. Organometallic chemistry on silicon surfaces: formation of functional monolayers bound through Si–C bonds. *Chem. Commun.* 12, 1051–1060.
- Cloarec, J.P., Deligianis, N., Martin, J.R., Lawrence, I., Souteyrand, E., Polychronakos, C., Lawrence, M.F., 2002. Immobilization of homooligonucleotide probe layers onto Si/SiO₂ substrates: characterization by electrochemical impedance measurements and radiolabelling. *Biosens. Bioelectron.* 17, 405–412.
- Cole, K.S., Cole, R.H., 1941. Dispersion and absorption in dielectrics. I. Alternating current characteristics. *J. Chem. Phys.* 9, 341.
- Fodor, S.P.A., Rava, R.P., Huang, X.C., Pease, A.C., Holmes, C.P., Adams, C.L., 1993. Multiplexed biochemical assays with biological chips. *Nature* 364, 555–556.
- Fritz, J., Cooper, E.B., Gaudet, S., Sorger, P.K., Manalis, S.R., 2002. Electronic detection of DNA by its intrinsic molecular charge. *Proc. Natl. Acad. Sci. U.S.A.* 99, 14142–14146.
- Gooding, J.J., 2002. Electrochemical DNA hybridization biosensors. *Electroanalysis* 14, 1149–1156.
- Heller, M.J., 2002. DNA microarray technology: devices, systems, and applications. *Annu. Rev. Biomed. Eng.* 4, 129–153.
- Higashi, G.S., Chabal, Y.J., Trucks, G.W., Raghavachari, K., 1990. Ideal hydrogen termination of the Si(1 1 1) surface. *Appl. Phys. Lett.* 56, 656–658.
- Kharitonov, A.B., Wasserman, J., Katz, E., Willner, I., 2001. The use of impedance spectroscopy for the characterization of protein-modified

- ISFET devices: application of the method for the analysis of biorecognition processes. *J. Phys. Chem. B* 105, 4205–4213.
- Korri-Youssoufi, H., Garnier, F., Srivastava, P., Godillot, P., Yassar, A., 1997. Toward bioelectronics: specific DNA recognition based on an oligonucleotide-functionalized polypyrrole. *J. Am. Chem. Soc.* 119, 7388–7389.
- Lin, Z., Strother, T., Cai, W., Cao, X., Smith, L.M., Hamers, R.J., 2002. DNA attachment and hybridization at the silicon(1 0 0) surface. *Langmuir* 18, 788–796.
- Linford, M.R., Fenter, P., Eisenberger, P.M., Chidsey, C.E.D., 1995. Alkyl monolayers on silicon prepared from 1-alkenes and hydrogen-terminated silicon. *J. Am. Chem. Soc.* 117, 3145–3155.
- Macdonald, R.J., 1987. *Impedance Spectroscopy: Emphasizing Solid Materials and Systems*, 1st ed. Wiley, Chapel Hill, NC.
- Memming, R., Schwandt, G., 1966. Potential distribution and formation of surface states at the silicon–electrolyte interface. *Surf. Sci.* 5, 97–110.
- Murphy, C.J., Arkin, M.R., Jenkins, Y., Ghatlia, N.D., Bossmann, S.H., Turro, N.J., Barton, J.K., 1993. Long-range photoinduced electron transfer through a DNA helix. *Science* 262, 1025–1029.
- Patolsky, F., Lichtenstein, A., Willner, I., 2001. Electronic transduction of DNA sensing processes on surfaces: amplification of DNA detection and analysis of single-base mismatches by tagged liposomes. *J. Am. Chem. Soc.* 123, 5194–5202.
- Popovich, N.D., Eckhardt, A.E., Mikulecky, J.C., Napier, M.E., Thomas, R.S., 2002. Electrochemical sensor for detection of unmodified nucleic acids. *Talanta* 56, 821–828.
- Souteyrand, E., Cloarec, J.P., Martin, J.R., Wilson, C., Lawrence, I., Mikkelsen, S., Lawrence, M.F., 1997. Direct detection of the hybridization of synthetic homo-oligomer DNA sequences by field effect. *J. Phys. Chem. B* 101, 2980–2985.
- Strother, T., Cai, W., Zhao, X., Hamers, R.J., Smith, L.M., 2000a. Synthesis and characterization of DNA-modified silicon(1 1 1) surfaces. *J. Am. Chem. Soc.* 122, 1205–1209.
- Strother, T., Hamers, R.J., Smith, L.M., 2000b. Covalent attachment of oligodeoxyribonucleotides to amine-modified Si(0 0 1) surfaces. *Nucleic Acids Res.* 28, 3535–3541.
- Vercoutere, W., Akeson, M., 2002. Biosensors for DNA sequence detection. *Curr. Opin. Chem. Biol.* 6, 816–822.
- Wagner, P., Nock, S., Spudich, J.A., Volkmuth, W.D., Chu, S., Cicero, R.C., Wade, C.P., Linford, M.R., Chidsey, C.D.E., 1997. Bioreactive self-assembled monolayers on hydrogen-passivated Si(1 1 1) as a new class of atomically flat substrates for biological scanning probe microscopy. *J. Struct. Biol.* 119, 189–201.
- Wang, J., 2002. Electrochemical nucleic acid biosensors. *Anal. Chim. Acta* 469, 63–71.
- Willner, I., Willner, B., 2001. Biomaterials integrated with electronic elements: en route to bioelectronics. *Trends Biotechnol.* 19, 222–230.
- Yu, C.J., Wang, H., Wan, Y., Yowanto, H., Kim, J.C., Donilon, L.H., Tao, C., Strong, M., Chong, Y., 2001. 2'-Ribose-ferrocene oligonucleotides for electronic detection of nucleic acids. *J. Org. Chem.* 66, 2937–2942.